



ELSEVIER

Journal of Chromatography A, 710 (1995) 309–321

JOURNAL OF
CHROMATOGRAPHY A

Systematic study of field and concentration effects in capillary electrophoresis of DNA in polymer solutions

Liouba Mitnik^{a,b}, Laurence Salomé^c, Jean Louis Viovy^{a,b}, Christoph Heller^{b,d,*}

^aLaboratoire de PhysicoChimie Théorique (URA CNRS 1382), Ecole Supérieure de Physique et de Chimie Industrielles de la Ville de Paris, 10 rue Vauquelin, 75231 Paris cedex 05, France

^bLaboratoire de PhysicoChimie Structurale et Macromoléculaire (URA CNRS 278), Ecole Supérieure de Physique et de Chimie Industrielles de la Ville de Paris, 10 rue Vauquelin, 75231 Paris cedex 05, France

^cCentre de Recherches Paul Pascal, CNRS, Avenue A. Schweitzer, 33600 Pessac, France

^dLaboratoire de Physique des Surfaces et Interfaces (URA CNRS 1379), Institut Curie, 11 rue Pierre-et-Marie Curie, 75005 Paris, France

First received 7 March 1995; revised manuscript received 21 April 1995; accepted 21 April 1995

Abstract

A systematic study of the separation of double-stranded DNA in hydroxypropylcellulose (HPC) with a molecular mass of 10^6 was undertaken, using a variety of concentrations (from 0.1 to 1%) and different electric fields (from 6 to 540 V/cm). The data show that at high polymer concentrations ($\geq 0.4\%$) and low fields, the separation mechanism is similar to that occurring in gels. The results are in good agreement with theoretical models, and in particular with a recently proposed theory for gels with a pore size smaller than the persistence length of DNA. For more dilute solutions and high fields, however, the separation pattern cannot be explained by existing theories. The existence of an original mechanism was confirmed by the direct observation of the conformation of double-stranded DNA molecules in the polymer solution by fluorescence videomicroscopy. Practical conclusions for the capillary electrophoretic separation of duplex DNA are drawn.

1. Introduction

Capillary electrophoresis (CE) has rapidly become a powerful and attractive separation technique because of its sensitivity, rapidity and the possibility of automation. The first separations of DNA by CE were performed in gels. However, the preparation of a gel-filled capillary is delicate. Air bubbles and inhomogeneities can be formed during the polymerization inside a capillary or during the electrophoresis. The structure of the gel may also vary along the

capillary. The use of polymer solutions instead of gels as a sieving medium avoids these problems and permits the experimental protocols to be simplified. It can be especially effective for large and flexible DNA molecules. Indeed, several studies yielded a good separation for DNA restriction fragments up to 23 kilo-base pairs (kbp) in different polymer solutions (e.g., [1,2]).

Some theoretical approaches that permit one to predict the separation and to evaluate the optimum separation conditions for different sizes of DNA molecules in polymer solutions of different concentrations have been proposed recently. The first theoretical description, to our knowl-

* Corresponding author.

edge, of DNA electrophoresis in polymer solutions was proposed by Grossman and Soane [3]. A more detailed theoretical model was developed by Viovy and Duke [4].

In order to check the conformity with experimental data and to establish if the models used for DNA electrophoresis in gels would be applicable to those in polymer solutions, we undertook a systematic study of the separation of double-stranded DNA in hydroxypropylcellulose (HPC) using a variety of concentrations and field strengths.

Also, we present here some data on the direct observation of DNA molecules during their migration in polymer solutions, obtained by epifluorescence microscopy. The observation of conformations of individual DNA molecules undergoing electrophoresis can be helpful in the understanding of migration mechanisms.

2. Theory

We recall in the following some proposed models for DNA separation in polymer solutions, in order to compare them with our experimental data.

2.1. Polymers

Three regimes of polymer solutions can be distinguished: dilute, semi-dilute and concen-

trated. However, for CE, only the dilute and semi-dilute regimes are relevant. The crossover between these regimes is characterized by the overlap concentration, c^* (see Fig. 1).

Other important parameters in the theory of polymer solutions are the square-averaged radius of gyration, $\langle R_g^2 \rangle$, and the screening length, ξ .

If the molecular mass, M_w , is known, a simple experimental way to determine the radius of gyration of a polymer is to measure the intrinsic viscosity $[\eta]$ in the dilute regime [5]:

$$[\eta] \approx 6.2R_g^3 N_A / M_w \quad (1)$$

where N_A is Avogadro's number. If the radius of gyration is known, this permits in turn the calculation of c^* , which is defined as

$$c^* \approx 3M_w / 4\pi N_A R_g^3 \approx 1.5[\eta]^{-1} \quad (2)$$

The screening length, ξ , is the distance above which the excluded volume interactions are screened by other chains. Grossman and Soane [3] proposed the use of this parameter as the effective "pore size" of the transient network. Viovy and Duke [4] proposed that the so-called "blob size", ξ_b (see Fig. 1), should be used instead. It is related to ξ by a universal prefactor [6]:

$$\xi_b = 2.86\xi = 1.43R_g(c/c^*)^{-3/4} \quad (3)$$

Therefore, this difference affects predictions quantitatively but not qualitatively.

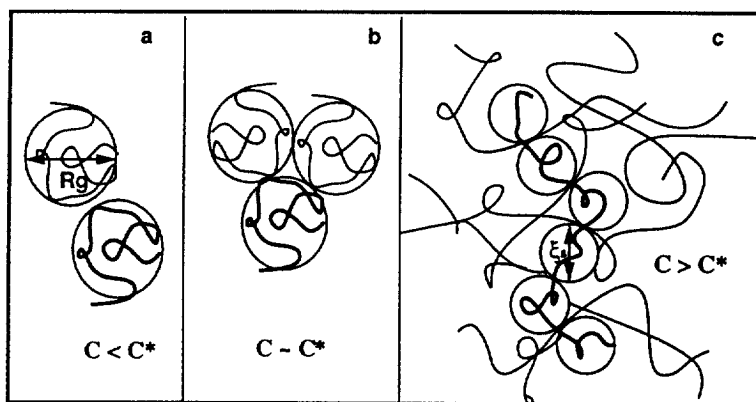


Fig. 1. Schematic representation of flexible polymers in solution. (a) Dilute solutions; (b) solutions at entanglement threshold c^* ; (c) semi-dilute solutions. One chain is drawn as a thick line for easier visualization. The small circles in c represent the "blobs" of size ξ_b .

2.2. Molecular mechanisms of size separation in polymer solutions

The first mechanism proposed for the description of gel electrophoresis, the Ogston model [7], assumes that the mobility of a particle is proportional to the fraction of the volume available to it in the gel. Using purely geometric arguments, Ogston derived an expression for the mobility of a globular particle in a random array of fibres:

$$\mu = \mu_0 \exp(-K_R C) \quad (4)$$

where μ_0 is the mobility in pure solvent, K_R is the retardation coefficient and C is the gel concentration. In order to apply the Ogston model to DNA separation, one assumes that the DNA migrates as a random coil. Then K_R should be

$$K_R \approx (R_{\text{DNA}} + r)^2 \quad (5)$$

where r is the radius of the gel fibres and R_{DNA} is the radius of gyration of the DNA molecule. Since the Ogston model is in principle applicable to rigid fibre-like obstacles, it is not obvious what should play the role of the “fibre radius”, r , in a solution of very flexible polymers. The molecular radius of HPC is of the order of 10–15 Å, i.e., negligible in comparison with the radius of gyration of DNA. Even in the opposite view, in which one considers that the blob size should play the role of the fibre radius, r would be much smaller than R_{DNA} for all experiments we performed, except for the smallest DNA in the most dilute solutions, where we shall see that there is virtually no separation. Therefore, r can be safely neglected in Eq. 5.

The Ogston model does not account correctly for the mobility of large DNA molecules in gels, so that a second type of model, the biased reptation model, was proposed. In the original biased reptation model (BRM), the DNA chain is assumed to thread its way, without changing its length, through a “tube” defined by the fibres (for a rigid mesh) or the “blobs” (for a flexible network) surrounding it. To facilitate the description of the DNA mobility, we introduce in the following two dimensionless parameters.

These are the mesh size normalized to the Kuhn length b of DNA, $\bar{\xi} = \xi_b/b$, and $\varepsilon_0 = Eq_k b/kT$, the electric potential energy per Kuhn length scaled to the thermal energy (q_k is the effective charge per DNA Kuhn segment).

The biased reptation model predicts that the electrophoretic mobility $\mu(N, E)$ in DNA gel electrophoresis is approximately related to the DNA molecular size N and the electric field E by [8]

$$\mu(N, E) \approx \frac{A}{N} + B(E) \quad (6)$$

with $B(E)$ proportional to E^β , where the exponent β equals 2 for low electric fields (i.e., far from saturation). When expressed in terms of molecular parameters, A and B should be $A \approx \bar{\xi}\mu_0/3$ and $B \approx \mu_0\varepsilon_0^2\bar{\xi}^4/6$, where μ_0 is the mobility in free solution.

For small molecular sizes, Eq. 6 predicts that $\mu(N)$ scales as $1/N$; for large sizes it predicts a plateau mobility.

This theory was recently improved by Duke et al. [9] to include the fluctuations in the length of the DNA molecule. This new model, called “biased reptation with fluctuations” (BRF), considers two different cases, as follows.

Mesh size larger than the Kuhn length of DNA ($\bar{\xi} > 1$)

For $\bar{\xi} > 1$, the BRF theory gives for the mobility μ_{rep}

$$\mu_{\text{rep}}/\mu_0 \approx \frac{\bar{\xi}}{3} [(1/N_k) + \varepsilon_0\bar{\xi}] \quad (7)$$

where N_k is the number of Kuhn segments. Therefore, the BRF model predicts two regimes for the mobility in constant field. For small DNA and/or a low electric field, the first term in Eq. 7 dominates (this regime is called: “reptation without orientation”); in this regime, the mobility varies as $\mu \propto 1/N_k$, and separation is possible. For a longer DNA and/or a higher electric field, a second regime, called “reptation with orientation”, is reached, where the second term in Eq. 7 dominates. This leads to a mobility independent of size. There is a crossover point between

these regimes, which marks the DNA size beyond which the separation power of electrophoresis becomes weaker and weaker and finally disappears. It occurs at

$$N_k^* \approx \varepsilon_0^{-1} \bar{\xi}^{-1} \quad (8)$$

These predictions are in good agreement with experimental results for DNA separation in agarose gels [10–12].

Mesh size smaller than the Kuhn length ($\bar{\xi} < 1$)

In this case, reptation without orientation still occurs below a critical size N_k^* , but the mobility in this regime should be independent of the pore size [4]:

$$\mu_{\text{rep}}/\mu_0 \cong \frac{1}{3N_k} \quad N_k < N_k^* \quad (9)$$

The theoretical values for the critical size and for the mobility beyond the crossover depend on ε_0 and $\bar{\xi}$:

(i) If $\varepsilon_0 < \bar{\xi}^{3/2}$:

$$\mu_{\text{rep}}/\mu_0 \cong \frac{\varepsilon_0}{3} \cdot \bar{\xi}^{3/2} \quad N_k > N_k^* \quad (10)$$

and $N_k^* \approx \varepsilon_0^{-1} \bar{\xi}^{-3/2}$.

(ii) If $\bar{\xi}^{3/2} < \varepsilon_0 < \bar{\xi}^{-1}$

$$\mu_{\text{rep}}/\mu_0 \cong \frac{\varepsilon_0^{2/5}}{3} \cdot \bar{\xi}^{12/5} \quad N_k > N_k^* \quad (11)$$

and $N_k^* \approx \varepsilon_0^{-2/5} \bar{\xi}^{-12/5}$.

(iii) Finally, if $\varepsilon_0 > \bar{\xi}^{-1}$:

$$\mu_{\text{rep}}/\mu_0 \cong \frac{\varepsilon_0^2}{3} \cdot \bar{\xi}^4 \quad N_k > N_k^* \quad (12)$$

and $N_k^* \approx \varepsilon_0^{-2} \bar{\xi}^{-4}$.

All the theories mentioned above take no account of the mobile nature of the obstacles. In order to apply them to entangled polymer solutions, Viovy and Duke [4] suggested that, even in the absence of self-reptation or Ogston sieving, there is a finite mobility related to constraint release (CR), i.e., the self-renewal of obstacles due to the motions of the polymers in the matrix. They calculated this mobility as

$$\mu_{\text{CR}}/\mu_0 \approx (c/c^*)^{-15/4} \bar{\xi} \quad (13)$$

and proposed that, to a first approximation (i.e., for low enough electric fields and large enough DNA), the overall mobility is approximately

$$\mu = \mu_{\text{rept}} + \mu_{\text{CR}} \quad (14)$$

3. Experimental

3.1. Viscosity measurements

The viscosity of aqueous solutions of HPC covering the concentration range 0.05–2% was determined using an Ubbelohde capillary viscometer positioned in a thermostatically controlled water-bath at $26.0 \pm 0.1^\circ\text{C}$. In this method, a liquid is allowed to flow through a fine-bore tube, and the viscosity is determined from the flow-rate, the gravitational pressure applied and the tube dimensions. Flow times for each solution were measured three times and readings agreed to within $\pm 0.05\%$.

The intrinsic viscosity $[\eta]$ obtained for HPC ($M_w 10^6$) (Aldrich) is 0.41 l/g. Using Eqs. 1 and 2, this yields a radius of gyration $R_g = 48$ nm and an overlap threshold $c^* = 0.37\%$. These values should be taken as orders of magnitude, however, because the sample is not monodisperse.

3.2. Instrumentation and chemicals

The DNA samples used were 1-kbp DNA ladder (Gibco BRL), $\phi\text{X174}/\text{HaeIII}$ digest (Gibco BRL) and $\text{Lambda}/\text{HindIII}$ digest (New England Biolabs) at concentrations ranging from 10 to 100 $\mu\text{g}/\text{ml}$.

Analysis of the DNA fragments was accomplished using an automated capillary electrophoresis instrument (P/ACE 2100; Beckman Instruments, Palo Alto, CA, USA). The runs were performed in 37 cm long (30 cm to the detector) coated capillary tubes of 100 μm I.D. (DB-1 and DB-17; J & W Scientific, Folsom, CA, USA).

The running buffer was $1 \times \text{TBE}$ (89 mM Tris-boric acid–2.5 mM EDTA) containing HPC ($M_w 10^6$) at different concentrations (0.1–

1%) and 10 μM ethidium bromide. All solutions were filtered and degassed before use.

The DNA samples were introduced into the capillary by electrokinetic injection at 175 V/cm for 10–30 s and separated at fields varying from 6 to 540 V/cm (negative polarity) at 25°C. For low electric fields, an external power supply was used instead of the built-in power supply. Detection was performed by UV absorption measurements at 254 nm.

3.3. Microscopic observations

An inverted microscope (Diaphot, Nikon) equipped for epifluorescence and with a Fluor 100 oil-immersion objective (Nikon) was coupled to a CCD camera with an image intensifier (Hamamatsu).

The following DNA samples were used: T4 phage DNA, 166 kbp (Amersham), and Lambda phage DNA, 48.5 kbp (Appligene). The DNA molecules were stained with an intercalating dye, oxazole yellow homodimer (YOYO, Molecular Probes), at a ratio of ca. 1 YOYO molecule per 10 bp. The DNA–polymer mixtures were placed between two cover-slips, which had been pre-treated by overnight incubation in 1% methylcellulose 4000 (Serva) followed by thorough rinsing with Milli-Q-purified water. This treatment renders electroosmosis negligible, as checked by the measurement of the velocity profile across the cell [13]. The whole assembly was mounted in a special electrophoresis chamber, adapted to the microscope.

4. Results and discussion

To establish the conformity of the theoretical approach mentioned above to experimental data, we undertook a series of mobility measurements of DNA fragments (size range from 72 bp to 23 kbp) in solutions of 0.1, 0.2, 0.4 and 1% HPC at different field strengths. Typical examples of separations under different conditions are given in Figs. 2 and 3.

4.1. Mobility versus molecular mass

Fig. 4 shows double logarithmic plots of mobility versus molecular mass. The results show the usual sigmoidal dependence of the mobility on molecular mass: medium-sized molecules are well resolved in all cases, whereas shorter and larger molecules assume nearly constant mobilities.

For 1% HPC (well above c^*), and 0.4% HPC (slightly above c^*) (Fig. 4c and d), the double logarithmic mobility versus molecular mass plot is very similar to that obtained by separation in gels [12], with a well defined reptation regime (slope = -1) and a plateau mobility for large DNA at low electric fields. At high electric fields, however, a separation is achieved for large DNA, a behaviour opposite to the biased reptation prediction, that the limit of separation decreases with increasing field (Fig. 3c and d).

For 0.1% and 0.2% HPC (i.e., below c^*) (Fig. 4a and b), the result is different. Even at low electric fields, the slope never reaches -1 , suggesting that in this case, reptation is not the main separation mechanism. Especially at higher field strengths, the mobility of the larger fragments never levels off totally, i.e. these fragments can still be separated.

4.2. Mobility versus electric field

The same data were replotted in order to demonstrate the dependence of the mobility on the electric field (Fig. 5). Again, the separation in 0.4% and 1% HPC is qualitatively very similar to that in gels (Fig. 5c and d): at low electric fields and/or low molecular mass, the mobility remains constant, i.e., is independent of the electric field, but it depends on size. Long chains (i.e., $N > N^*$), in contrast, show a linear $\log(\text{mobility})$ versus $\log(\text{electric field})$ dependence. At 1% HPC, the slope is 0.4, in excellent agreement with Eq. 11.

For 0.1% and 0.2% HPC (Fig. 5a and b), the picture is qualitatively similar, but the slope of the mobility versus electric field plot for the large molecules is even lower, with a value of about 0.2–0.3. Unsurprisingly, this behaviour is not

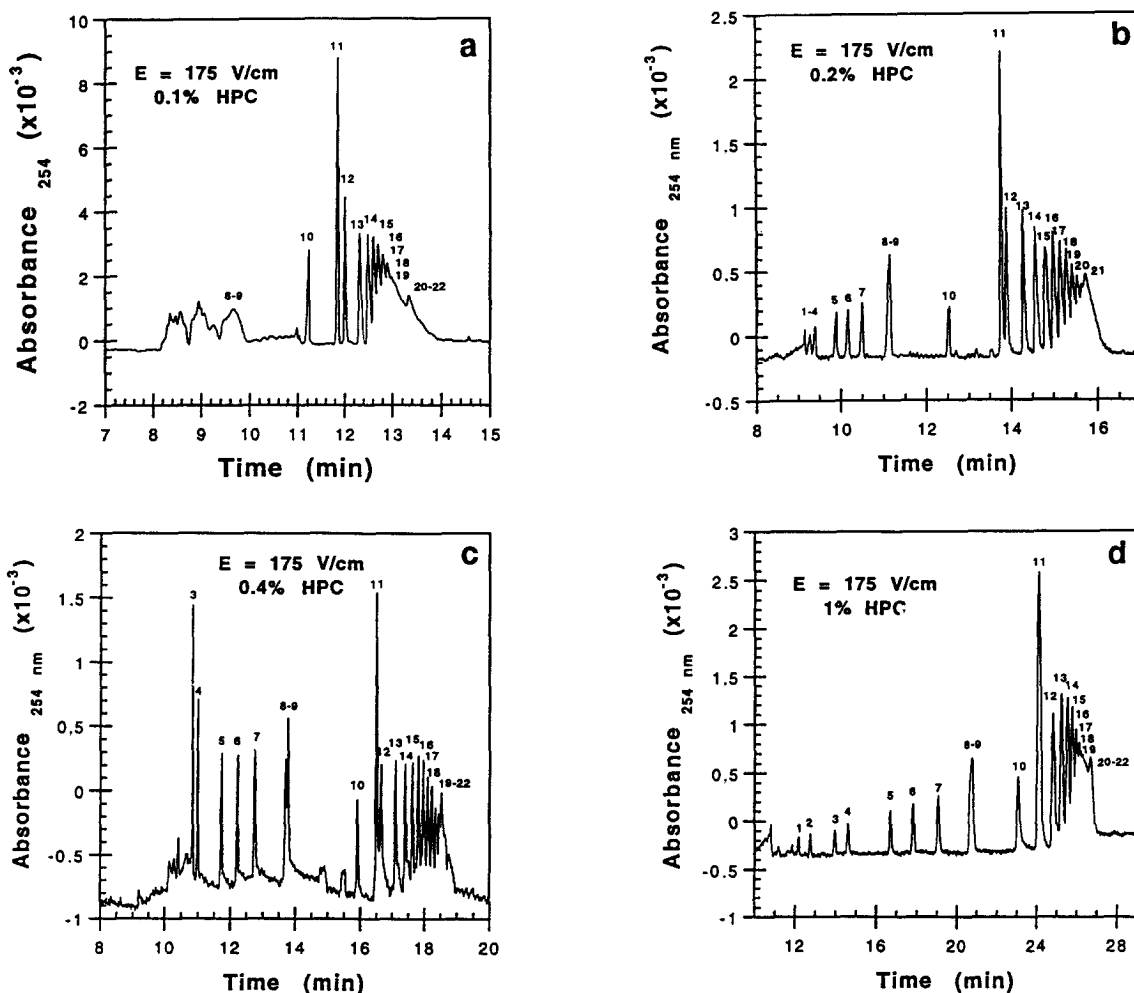


Fig. 2. Capillary electrophoresis of 1-kbp ladder ranging in size from 134 to 12 216 bp at different HPC concentrations, but with the same electric field: (a) 0.1%, (b) 0.2%, (c) 0.4% and (d) 1% HPC in 89 mM Tris–89 mM boric acid–2.5 mM EDTA–10 μ M etidium bromide. Common conditions: coated capillary, DB-17; distance to detector, 30 cm; total length, 37 cm; I.D., 100 μ m; field strength, 175 V/cm; temperature, 25°C. Peaks: 1 = 134; 2 = 154; 3 = 201; 4 = 220; 5 = 298; 6 = 344; 7 = 394; 8 = 506; 9 = 517; 10 = 1018; 11 = 1635; 12 = 2036; 13 = 3054; 14 = 4072; 15 = 5090; 16 = 6108; 17 = 7126; 18 = 8144; 19 = 9162; 20 = 10 180; 21 = 11 198; 22 = 12 216 bp.

predicted by the reptation theory, since at this concentration, the HPC used in these experiments is not fully entangled.

4.3. Reptation plot

Recently, a new representation of electrophoretic data as mobility times molecular size versus molecular size was proposed [8]. The existence of straight lines converging to a single point on

the ordinate is expected to provide a “signature” of reptation behaviour, and allow a direct evaluation of the parameters entering mobility equations of the type of Eq. 6 or 7. On plotting our data using this so-called “reptation plot” [8], we indeed obtain straight lines, which seem to converge well towards a single point on the ordinate (not shown). Strikingly, this is true even for the data obtained at low HPC concentrations, for which the log–log representation (Fig.

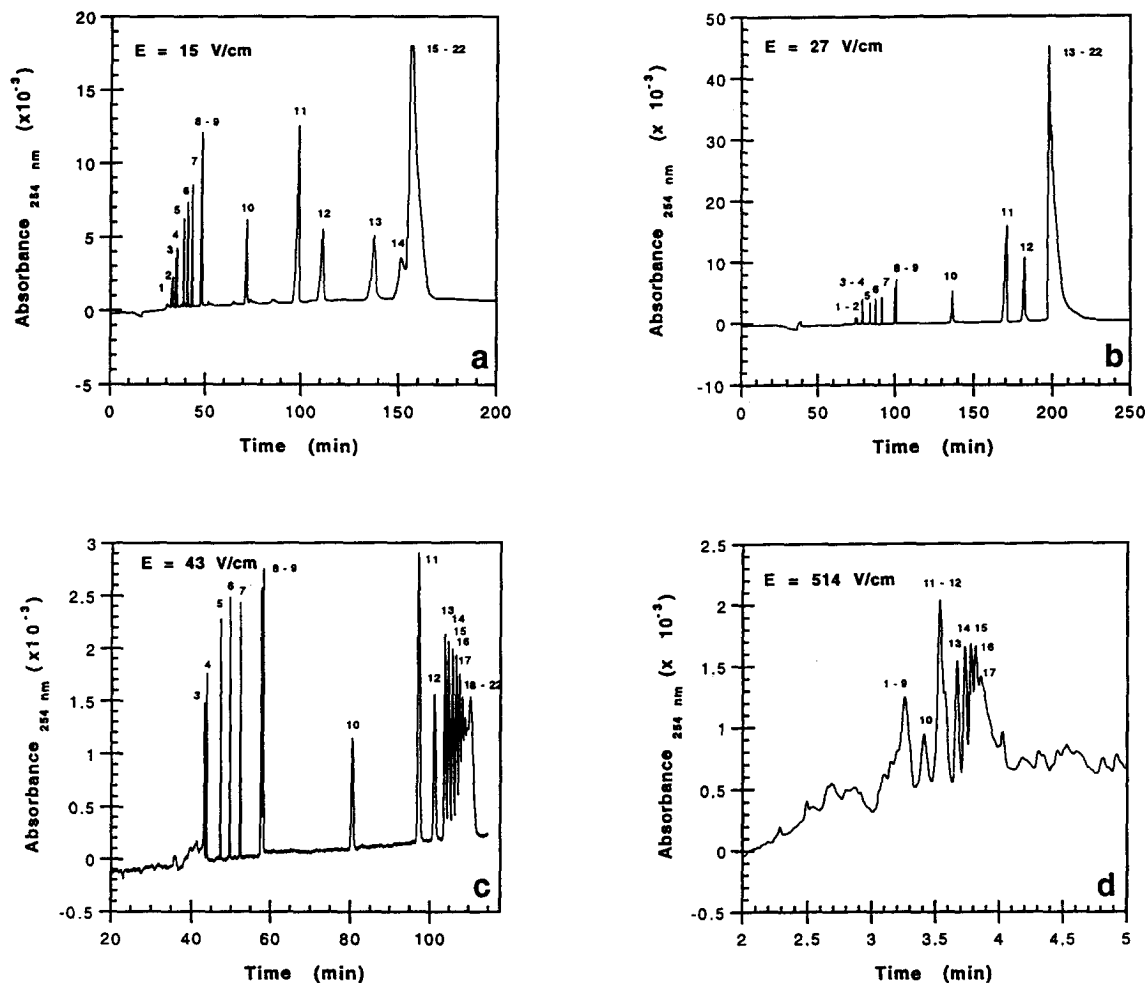


Fig. 3. Capillary electrophoresis of 1-kbp ladder under different electric field strengths, but at same polymer concentration (0.4% HPC), in 89 mM Tris–89 mM boric acid–2.5 mM EDTA–10 μ M ethidium bromide. Conditions and peaks as in Fig. 2.

5a and b) provides no domain where the mobility is inversely proportional to the size. We conclude that the reptation plot is actually not a very accurate way of checking for reptation behaviour, probably because it puts relatively too much weight on data corresponding to the largest DNA. Fig. 6 presents a log–log plot of the slopes of the reptation plots, $B(E)$, versus the electric field which allows us to calculate the parameter β [8]. For the 1% HPC solution we obtain a slope of 0.4, in good agreement with the value obtained using the more classical log–log plot (Fig. 5d). For the 0.4%, 0.2% and 0.1%

HPC solutions, the slope is 0.3, 0.27 and 0.07, respectively. In no case could we observe a square dependence of $B(E)$ on the field, as would be predicted by the biased reptation model without fluctuations (Eq. 6).

4.4. Ogston model

We also plotted the data for the lowest and highest HPC concentrations (0.1% and 1%) as log μ versus N (Fig. 7), in order to compare them with the predictions of the Ogston model. In both cases, considerable curvature is obtained

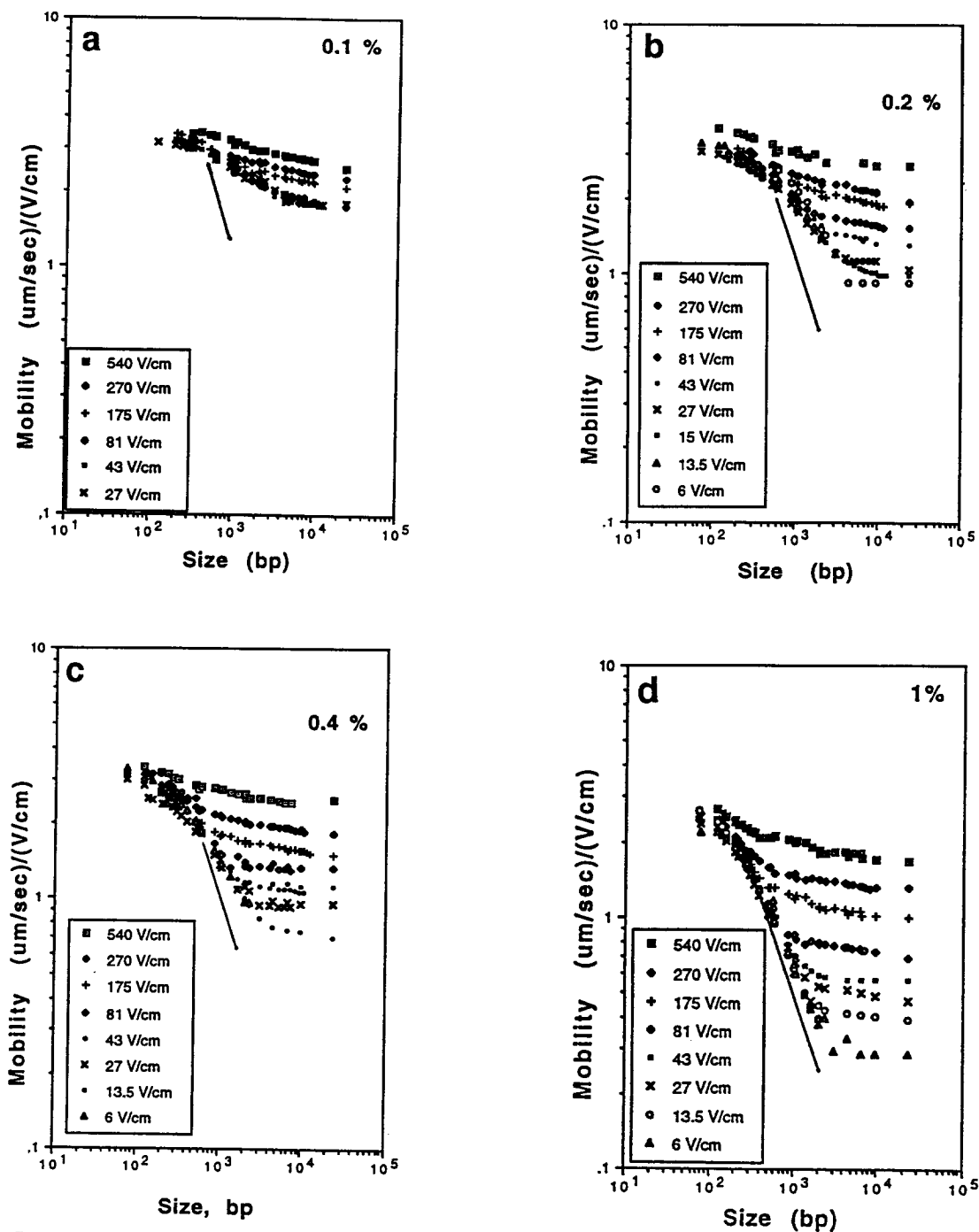


Fig. 4. Dependence of the electrophoretic mobility of linear double-stranded DNA fragments on the molecular mass in (a) 0.1, (b) 0.2, (c) 0.4 and (d) 1% HPC solutions at different electric field strengths in $1 \times$ TBE containing $10 \mu\text{M}$ ethidium bromide at 25°C . The lines have a slope of -1 .

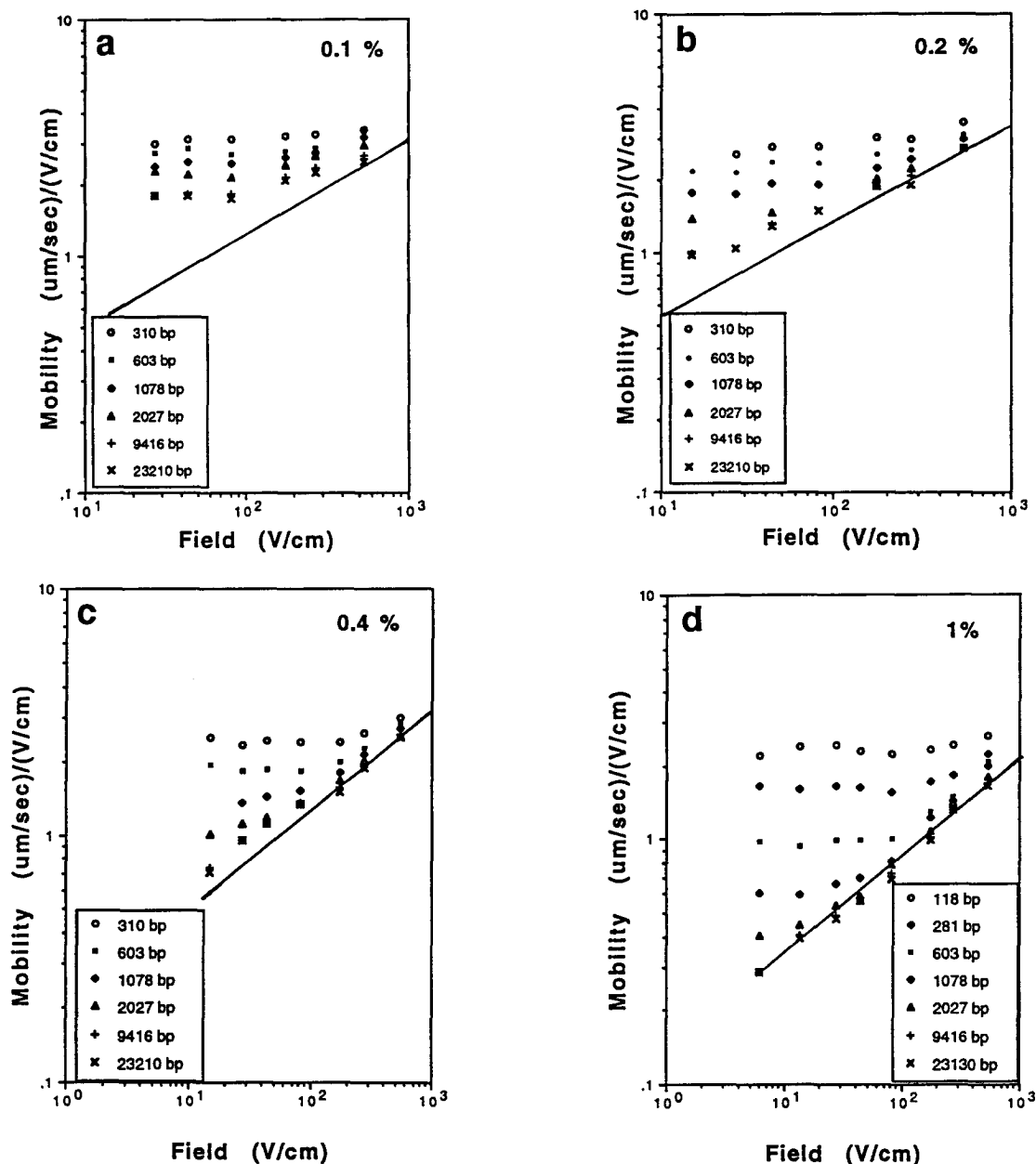


Fig. 5. Dependence of the electrophoretic mobility of linear double-stranded DNA fragments on the electric field in (a) 0.1, (b) 0.2, (c) 0.4 and (d) 1% HPC. The lines have a slope of 0.4. Same conditions as in Fig. 4.

above a critical size smaller than 1 kbp, confirming that the Ogston model does not describe the mobility of DNA better in polymer solutions than it does in gels. Only the mobility of the smallest fragments yields approximately a

straight line. The deviation from linearity occurs at around 500 bp in 1% HPC and around 1 kbp in 0.1% HPC solution.

It is worth pointing out that, even for small DNA, only the data obtained at 1% HPC show a

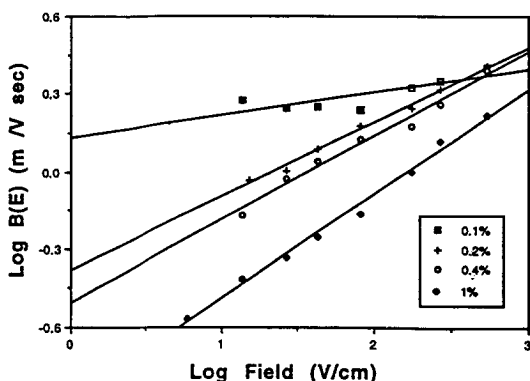


Fig. 6. Log-log plot of $B(E)$ versus electric field.

mobility independent of the electric field (as it should be according to the Ogston model). For low concentrations, the mobility depends on the electric field for large fields. This behaviour, which is not predicted by the Ogston model, suggests that the mobility of the DNA may in part be determined by the mobile nature of the obstacles (“constraint release”).

4.5. Quantitative comparison with reptation and constraint release models

One important advantage of reptation and constraint release models is that they involve only molecular parameters with a clear significance. The mobility can in principle be predicted

without any adjustable parameter, using only independently measured quantities. This is obviously an ambitious goal, because theoretical modelling always involves oversimplifications. However, we believe that a semi-quantitative agreement obtained in such conditions is a more stringent and more convincing test than a quantitative agreement obtained with several adjustable parameters.

For the BRF, four parameters are needed: the mobility of the DNA in free solution, μ_0 , its Kuhn length (twice the persistence length), b , the effective charge of the DNA per Kuhn segment, q_k , and the pore size of the separating matrix, ξ .

The Kuhn length of duplex DNA varies with the ionic strength of the buffer. In $1 \times$ TBE, it is equal to 100 ± 20 nm (or around 300 base pairs). From several experiments, and in particular from videomicroscopic measurements of chain stretching under the influence of an electric field [14], the effective charge is now evaluated as typically $0.1 \pm 0.05 e^-$ per base pair. Using the definition of ε_0 , this yields $\varepsilon_0/E \approx 1.2 \cdot 10^{-2}$ cm/V.

In our case, the effective pore sizes ξ_b , evaluated using Eqs. 2 and 3, are 185, 110, 65 and 32 nm for 0.1, 0.2, 0.4 and 1% HPC, respectively. The corresponding values of $\bar{\xi}$ are 1.85, 1.10, 0.65 and 0.32. This suggests that for $c > 0.2\%$, our experiments correspond to the regime in

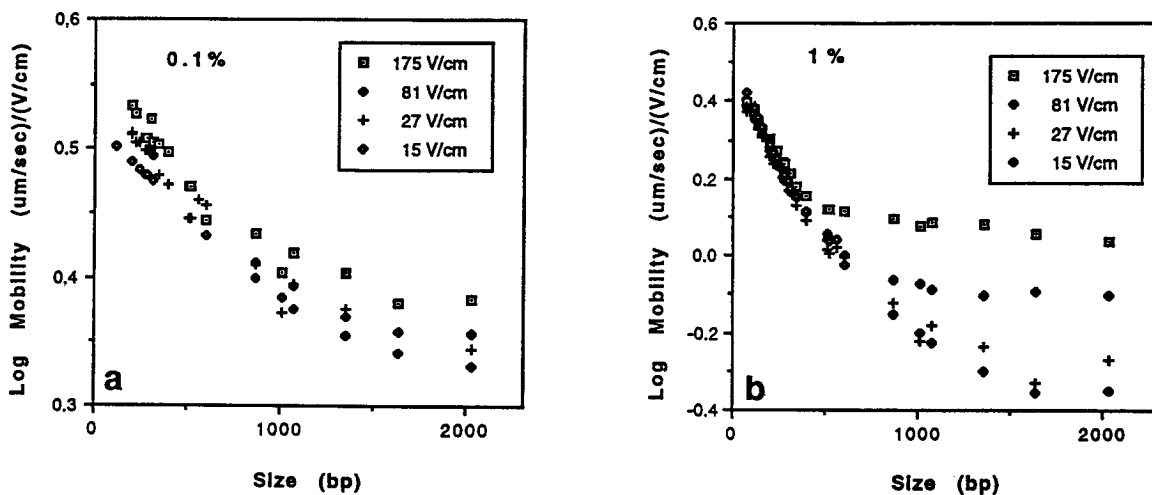


Fig. 7. Log-linear plot of the mobility of DNA versus molecular size. (a) 0.1% and (b) 1% HPC.

which the pore size is smaller than the Kuhn length of DNA (Eqs. 9–12).

The absolute mobility in free solution, μ_0 , was evaluated from experiments by Olivera et al. [15]. In 1×TBE, it should be around $3 \pm 0.5 \cdot 10^{-4} \text{ cm}^2/\text{V}\cdot\text{s}$. Inserting this values in Eq. 9, one obtains, in the linear regime (i.e. $N_k < N_k^*$),

$$\mu_{\text{theor,lin}} \approx (1/N_k) \cdot 10^{-4} \text{ cm}^2/\text{V}\cdot\text{s} \quad (15)$$

In the double logarithmic mobility versus size plot, this regime can be associated with the portion in which the mobility is independent of field and inversely proportional to size (slope -1). In 1% solutions, where gel electrophoresis theories are most likely to apply, we find from Fig. 4d,

$$\mu_{\text{exp,lin}} \approx (1/N_k) \cdot 2 \cdot 10^{-4} \text{ cm}^2/\text{V}\cdot\text{s} \quad (16)$$

Considering that the numerical prefactors in the reptation theory are not well known, this is a fairly good agreement.

In the non-linear regime (i.e. $N_k > N_k^*$), the theory predicts a plateau mobility, which is indeed observed. The field dependence of this plateau when $\bar{\xi} < 1$ is expected to be complex, as can be seen from Eqs. 10–12. Using the absolute parameters for μ_0 , ε_0/E and $\bar{\xi}$ determined independently, one expects the mobility to be proportional to E when $\varepsilon_0 < \bar{\xi}^{3/2}$ (i.e. $E < 45 \text{ V/cm}$ at 0.4% and $E < 15 \text{ V/cm}$ at 1% HPC), proportional to $E^{2/5}$ for $\bar{\xi}^{3/2} < \varepsilon_0 < \bar{\xi}^{-1}$ (i.e. $45 \text{ V/cm} < E < 130 \text{ V/cm}$ at 0.4% and $15 < E < 240 \text{ V/cm}$ at 1% HPC) and proportional to E^2 (i.e. $E > 130 \text{ V/cm}$ and $E > 240 \text{ V/cm}$, respectively). Experiments (for 1% HPC) show that the mobility is proportional to $E^{0.4}$ for the whole range, i.e., from 6 to 540 V/cm (Fig. 5d). This is in reasonable agreement with the theoretical predictions.

Finally, it is worth pointing out that the absolute values of the mobility of long DNA that can be predicted from Eq. 11 using the above-mentioned values of ε_0 , $\bar{\xi}$ and μ_0 (not shown) are about three (for 1% HPC) to ten times (for 0.4% HPC) smaller than the measured values (Fig. 5c and d). It is unlikely that this discrepancy is due only to the poor knowledge of

prefactors in the theory, because the BRF model was able to predict the absolute mobility in agarose gel electrophoresis within a factor of about two [16]. More probably, this discrepancy is due to the labile nature of the obstacles in a polymer solution as compared with permanent gels, i.e., to constraint release processes. Viovy and Duke [4] proposed a linear theory of constraint release and derived an expression for the constraint release mobility in terms of molecular parameters (Eq. 13). When the values of c/c^* and $\bar{\xi}$ are introduced into this expression, however, one finds a mobility which is still smaller than that observed experimentally, and which depends much more strongly on the concentration than observed experimentally. Moreover, the constraint release mobility predicted by the theory is independent of the field strength and of the molecular mass of the DNA, whereas the measured mobility depends on E and also depends weakly on the DNA size for strong fields. We conclude that the constraint release theory used in the currently available models [4], which neglects deformations of the polymer matrix by the DNA, and coupling between the DNA dynamics and the matrix dynamics, cannot account for the observed discrepancy between the predicted and measured values of the absolute mobility of large DNA. To try to understand the actual mechanism at play in these separations, we turned to a very different set-up, in which the molecules themselves can be observed in the course of migration.

4.6. Microscopic observations

The existence of an original migration mechanism at a polymer concentration around c^* was confirmed by the direct videomicroscopic observation of DNA molecules in the course of migration. In free liquid, molecules migrate in a random coil conformation (Fig. 8b) essentially identical with that which they adopt in the absence of field (Fig. 8a). Strikingly, however, at concentrations below c^* , molecules can become significantly extended, and often adopt U-shapes reminiscent of those observed in real gels [17] (Fig. 9). The DNA molecules progressively slide

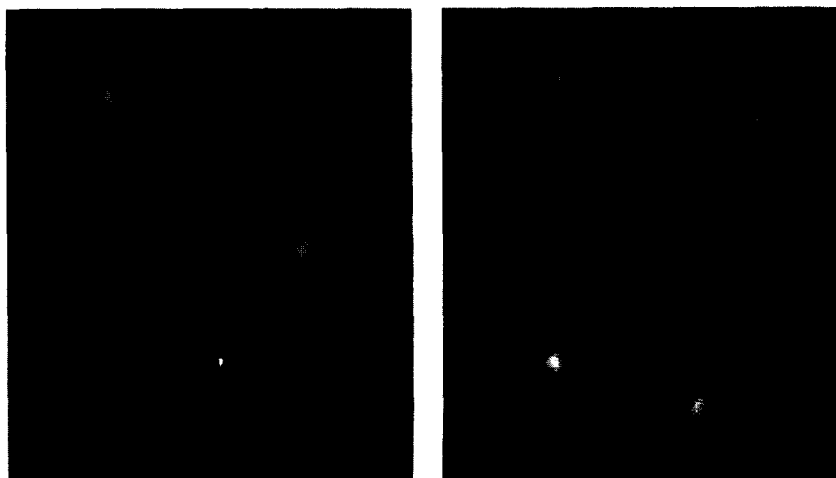


Fig. 8. Microscopic observation of Lambda DNA molecules. Conditions: (left) conformation in free liquid in the absence of field; (right) migration in free liquid at $E = 10$ V/cm. In both cases, the DNA molecules adopt a random coil conformation.

along their own contour to yield J-shapes, and finally adopt an extended conformation again. There are two differences between the U shapes observed in solutions below c^* and in gels, however. First, the conformations in polymer solutions are more open than in gels. Second, the top of the U (or the “pulley” around which the DNA slides) is itself moving downfield while the DNA disengages from it, whereas in gels it is

immobile. The relative velocity of this downfield motion compared with that of the sliding motion decreases when the concentration of the polymer solution is increased. These qualitative observations are compatible with a mechanism in which the DNA molecule has to slide its way among the polymer obstacles, but also deforms and drag them along at the same time. This would also explain why the mobility observed in polymer

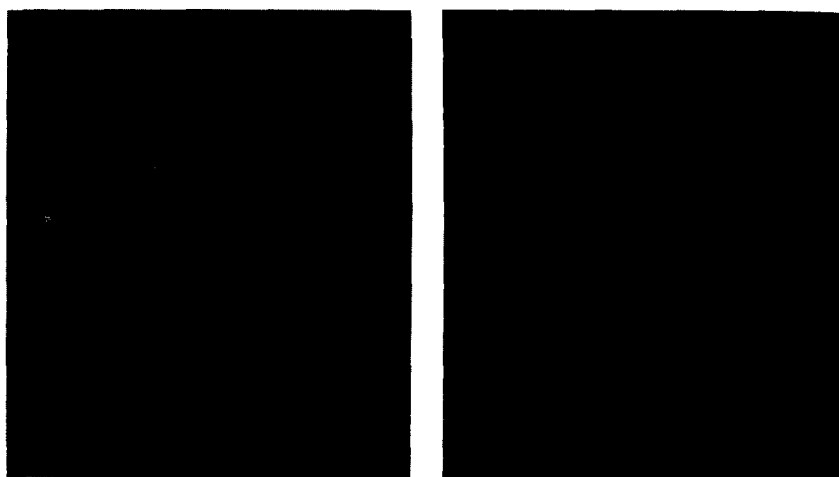


Fig. 9. Microscopic observation of Lambda DNA molecules in a 0.2% HPC solution at $E = 10$ V/cm. The two photographs display the same portion of the cell at different times, showing examples of U-shapes, J-shapes and extended conformations adopted by the molecules.

solutions is larger than predicted by the linear reptation and constraint release models, and why it depends on the electric field (the stronger is the field, and the more the DNA is able to deform the matrix). This dragging along of polymers is similar to the “entanglement coupling” mechanism recently proposed by Barron et al. [18] for dilute solutions, but the additional curvilinear sliding of DNA complicates the mechanism.

5. Conclusions

We performed a systematic study of the migration and separation properties of DNA in a high-molecular-mass water-soluble polymer, hydroxypropylcellulose. This study considered the effect of concentration, going well into the entangled regime, and the effect of the field strength over two orders of magnitude. The results were compared with theoretical predictions. For the first time in CE in non-gel media, we could observe regimes qualitatively consistent with the migration mechanism known in gel electrophoresis [biased reptation with fluctuations (BRF)]. This is probably due to the fact that we used an unusually large polymer at a high concentration (about four times the overlap concentration, c^*) and low electric fields. We demonstrated that such highly entangled solutions are able to provide a better resolution than more dilute ones, although on a narrower range of sizes. Our results also confirm that even unentangled solutions can separate DNA, as demonstrated recently by Barron et al. [18]. The choice of highly entangled or dilute solutions for a given application, essentially depends on the range of sizes to be separated and on the quality of the resolution required: dilute solutions are better for low resolution over a wide range, and entangled solutions for high resolution over a narrow range. Our results also point out the limited success of existing theories for describing electrophoresis in polymer solutions and suggest a new mechanism of migration, which combines a sliding of DNA molecules around obstacles and a dragging of these obstacles by the DNA.

Theoretical work is in progress to describe the mobility of DNA in unentangled or weakly entangled polymer solutions [19].

Acknowledgements

This work was partly supported by Beckman France and by an EC (DG XII) “Human Genome” grant, No. CT93-0018. We thank Xavier Chaudot and Emmanuel Nonnet for their assistance.

References

- [1] M. Strega and A. Lagu, *Anal. Chem.*, 63 (1991) 1233.
- [2] M. Chiari, M. Nesi and P.G. Righetti, *J. Chromatogr. A*, 652 (1993) 31.
- [3] P.D. Grossman and D.S. Soane, *Biopolymers*, 31 (1991) 1221.
- [4] J.L. Viovy and T.A.J. Duke, *Electrophoresis* 14 (1993) 322 (note that Eqs. 10 and 12 in this paper contain erroneous numerical prefactors; Eqs. 1 and 2 in the present paper contain the correct prefactors).
- [5] M. Doi and S.F. Edwards, *The Theory of Polymer Dynamics*, Clarendon Press, Oxford, 1986.
- [6] D. Broseta, L. Leibler, A. Lapp and C. Strazielle, *Europhys. Lett.*, 2 (1986) 733.
- [7] A.G. Ogston, *Trans. Faraday Soc.*, 54 (1958) 1754.
- [8] P. Mayer, G.W. Slater and G. Drouin, *Appl. Theor. Electrophoresis*, 3 (1993) 147.
- [9] T.A.J. Duke, J.L. Viovy and A.N. Semenov, *Biopolymers*, 34 (1994) 239.
- [10] W.L. Fangman, *Nucleic Acids Res.*, 3 (1978) 653.
- [11] H. Hervet and C. Bean, *Biopolymers*, 26 (1987) 727.
- [12] C. Heller, T. Duke and J.L. Viovy, *Biopolymers*, 34 (1994) 249.
- [13] L. Mitnik, J.L. Viovy and L. Salomé, paper presented at the 33rd IUPAC Microsymposium on Optics and Dynamics of Polymers, Prague, July 1993.
- [14] S.B. Smith and A.J. Bendich, *Biopolymers*, 29 (1990) 1167.
- [15] B.M. Olivera, P. Baine and N. Davidson, *Biopolymers*, 2 (1964) 245.
- [16] M.S. Hutson, G. Holzwarth, T. Duke and J.L. Viovy, *Biopolymers*, 35 (1995) 297.
- [17] C. Bustamante, *Annu. Rev. Biophys. Biophys. Chem.*, 20 (1991) 415.
- [18] A.E. Barron, D.S. Soane and H.W. Blanch, *J. Chromatogr. A*, 652 (1993) 3.
- [19] G.W. Slater, et al., in preparation.